Proc. of the 8th International Symposium on Geotechnical Safety and Risk (ISGSR)
Edited by Jinsong Huang, D.V. Griffiths, Shui-Hua Jiang, Anna Giacomini and Richard Kelly

doi: 10.3850/978-981-18-5182-7_11-023-cd

ISGSR 2022

Reliability Analysis of Unsaturated Soil Slope Stability Using Spatial Random Fields-Based Bayesian Method

C. H. Wang[1],H. D. Du[2],S. T. Hu[3]

[1]Department of Civil Engineering,Shanghai University/333 Nanchen Road, Shanghai 200444, China
E-mail: ch_wang@shu.edu.cn
[2]Department of Civil Engineering, Shanghai University/333 Nanchen Road, Shanghai 200444, China
E-mail: duhaodong@shu.edu.cn
[3]Department of Civil Engineering, Shanghai University/333 Nanchen Road, Shanghai 200444, China
E-mail: hushitao@shu.edu.cn

Abstract: Rainfall and water level change are two main factors causing failure of reservoir slopes. Thus soil-fluid mechanics is applied with the fluctuation of groundwater table. However, many geotechnical parameters needed for the analysis are highly varied. Spatial random fields-based Bayesian method is proposed, which can systematically assimilate prior knowledge, borehole test data and long-term monitoring data to obtain posterior distributions. There are three major components of the method. They include unsaturated soil-fluid coupling mechanics, spatial multivariate discretization, and subset Monte-Carlo simulation of reliability analysis. The approach is applied to the Shiliushubao slope of the Three Gorges Reservoir area, which is located 9.0km downstream of the Badong County in Hubei Province, China. Results prove that the updated key geotechnical parameters will quantitatively predict the geohazard of landslide, especially for unsaturated soil slope that suffers an unprecedented heavy rainfall subject to low reservoir water level in the summer. According to the conditions of heavy rainfall and rapid rise and fall of the Yangtze River water level in 2020, the reliability analysis of the old Shiliushubao landslide is carried out in the Three Gorges Reservoir area.The results for the two different conditions both indicate that the safety factor of the slope stability is low, but the reliability index meets the minimum requirement of 2.70 according to the specification. None of the additional reinforcement measures are required.

Keywords:Geotechnical parameters· spatial random fields· Bayesian method· Unsaturated soil slope· Reliability analysis

1 Introduction

Heavy rainfall and water level fluctuation are two of the main factors contributing to reservoir landslides (De Vita *et al.*, 1998; Huang *et al.*, 2016). Many landslides were reactivated by the first impoundment of the Three Gorges Reservoir, China (Jian *et al.*, 2014). Early warning system of long-term monitoring data has been used to prevent and mitigate geohazards. However, it is difficult to make quantitative predictions on the re-activation of reservoir landslides. Cai *et al.* (2017) analyzed the spatial variability of hydraulic conductivity and shear strength of an infinite slope during groundwater recharge. Zheng *et al.* (2017) predicted the mechanical behaviors of an embankment using laboratory data and field measurements. Lo and Leung (2019) studied the spatial variability of subsurface soil for improving prediction of braced excavation response with a Bayesian method. However, there was only one geotechnical parameter taken into account.

The early literature was concentrated on Spatial Random Field (SRF) of univariate. It is an innovative idea that denotes the key geotechnical parameters as multivariate SRFs, *e.g.*, effective cohesion, c', effective internal friction angle, φ', Young's modulus, E and saturated hydraulic conductivity, k_s of an unsaturated slope. Spatially correlated geotechnical parameters will be calibrated by assimilating prior knowledge, borehole testing data, long-term monitoring data, and soil-fluid coupling mechanics within Bayesian framework. Furthermore, reactivation of once failed reservoir slope will be predicted under an unprecedented heavy rainfall for the upcoming summer.SRFs-based Bayesian method is organized as follows. Soil-fluid coupling mechanics of unsaturated slope is presented as the first step, which is followed by SRFs, Bayesian method and reliability analysis. This approach is applied to Shiliushubao slope in the Three Gorges Reservoir area, China. It was a well-known failed soil slope in the year 1975. Potential geohazards of landslide reactivation are taken into account with the calibrated key geotechnical parameters.

2 Soil-fluid coupling mechanics

Soil-fluid coupling mechanics of an unsaturated slope consist of three basic components, and these components include transient seepage analysis under rainfall infiltration and reservoir water level fluctuation, effective shear strength analysis, and stability analysis of potential landslide.

2.1 Transient seepage analysis

Soil-Water Characteristic Curve (SWCC) and Hydraulic Conductivity Function (HCF) will make a substantial contribution to solve transient flow function (Richards, 1931). Many analytical models have been developed to describe the SWCC and HCF. For the purpose of the current study, Van Genuchten's model (Van Genuchten, 1980) is shown in Eq.(1),

$$\begin{aligned} \Theta_{\mathrm{w}} &= \frac{\theta_{\mathrm{w}}-\theta_{\mathrm{r}}}{\theta_{\mathrm{s}}-\theta_{\mathrm{r}}} = \left[\frac{1}{1+\left\{\alpha\left(u_{\mathrm{a}}-u_{\mathrm{w}}\right)\right\}^{n_{\mathrm{s}}}}\right]^{m} \\ k &= k_{\mathrm{s}}\Theta_{\mathrm{w}}^{1/2}\left[1-\left(1-\Theta_{\mathrm{w}}^{1/m}\right)^{m}\right]^{2} \end{aligned} \tag{1}$$

where Θ_{w} is the normalized volumetric water content, θ_{s} is the saturated volumetric water content, θ_{r} is the residual volumetric water content, u_{a} is the pore air pressure, u_{w} is the pore water pressure, k_{s} is the saturated hydraulic conductivity, and unsaturated hydraulic conductivity k is determined by the function of HCF. α, m and n_{s} are the constant coefficients of SWCC.

2.2 Shear strength of unsaturated soil

Effective stress σ' of unsaturated soil is derived from three variables, total stress σ, pore air pressure u_{a}, and suction stress σ_{s} (Lu *et al.*, 2010),the effective shear strength of unsaturated soil is obtained as depicted in Eq.(2),

$$\tau_{\mathrm{f}} = c' + \left(\sigma - u_{\mathrm{a}}\right)\tan\varphi' + \Theta_{\mathrm{w}}\left(u_{\mathrm{a}} - u_{\mathrm{w}}\right)\tan\varphi' \tag{2}$$

where σ_{s} is expressed by a function of the matric suction $u_{\mathrm{a}}-u_{\mathrm{w}}$, τ_{f} denotes the effective shear strength, c' is the effective cohesion, and φ' is the effective internal friction angle.

2.3 Stability analysis of unsaturated slope

Factor of Safety (FOS) of unsaturated slope stability is analyzed by Morgenstern-Price (M-P) limit equilibrium method. Static balance equation of F_{s} is given out in Eq.(3),

$$F_{\mathrm{s}} = \frac{\sum_{n}(c_i' + \sigma_i'\tan\varphi_i')l_i}{\sum_{n}(W_i + Y_{i-1} + Y_i)\sin\alpha_i + \sum_{n}(X_i - X_{i-1})\cos\alpha_i} \tag{3}$$

where W_i is the weight of the slice i, X_{i-1} and X_i are the horizontal inter-slice forces, Y_{i-1} and Y_i are the vertical inter-slice forces, thrust force is $E_i=\sqrt{X_i^2+Y_i^2}$, α_i is the slope angle of the slice i, and l_i is the arc length of the slice i, $i=1,\ldots,n$.

3 SRFs-based Bayesian method

SRFs-based Bayesian method is employed to analyze uncertainty propagation of geotechnical parameters. In this case, the outer loop will calibrate the key geotechnical parameters utilizing Bayesian theorem, which can assimilate prior knowledge, borehole testing data and long-term monitoring data through soil-fluid coupling mechanics. Furthermore, the inner loop will take out the stochastic analysis of slope stability under the posterior distributions.

3.1Spatial random fields

Soil-fluid coupling analysis customarily involves multiple geotechnical parameters, such as the strength, deformation and seepage properties, in which case the Random Variable (RV) ignores spatial variability, where the Coefficient of Variation (COV), $\delta = v/\mu$, synthesizes the randomness, μ denotes the mean value, and v is the Standard Deviation (SD).

SRFs can take randomness into account and emphasize spatial variability. In addition to the mean values $\boldsymbol{\mu}$ and SD values $\boldsymbol{v}$, SRFs use the correlation function(Matheron and Armstrong, 1963) to depict the spatial variability as shown in Eq. (4) ,

$$\rho_{i,i}(h) = \frac{E\{[\psi_i(x+h)-\mu_i]\cdot[\psi_i(x)-\mu_i]\}}{v_i^2} \tag{4a}$$

$$\rho_{i,j}(h) = \frac{E\{[\psi_i(x+h)-\mu_i]\cdot[\psi_j(x)-\mu_j]\}}{v_i v_j} \tag{4b}$$

where $\rho_{i,i}(h)$ is the autocorrelation function, $i=1,...,m$, m is the number of the key geotechnical parameters,cross-correlation function $\rho_{i,j}(h)\ (i,j=1,...,m,i\neq j)$ depicts mutually spatial variation of SRFs. It may assume, $\rho_{i,j}(h)=\rho_{j,i}(h)$.

Exponential model is adaptive for long-range correlated SRFs, while Gaussian model can depict the reversed curves of a correlation function. As suggested by Vanmarcke (1977), Spherical model has the advantages of conciseness and robustness. Hence Eq.(5) is used into application,

$$\rho(h)=\begin{cases}1-[1.5(h/a_1)-0.5(h/a_1)^3] & 0\le h\le a_1\\ 0, & h>a_1\end{cases} \tag{5}$$

where $\rho(h)$ is the correlation coefficient between lag distance h, and a_1 is the primary correlation range.

Three-dimensional heterogeneity is measured by the weighted lag distance h (Wang, *et al.*, 2017) as shown Eq.(6),

$$h=\sqrt{(\frac{h_1}{\eta_1})^2+(\frac{h_2}{\eta_2})^2+(\frac{h_3}{\eta_3})^2} \tag{6}$$

where η_1 is kept in constant, 1.0 for the primary correlation range a_1(*e.g.*, parallel with the slope surface), η_2 is the range ratio of the second correlation range a_2 (*i.e.*, perpendicular to the primary range in the vertical plane) divided by a_1, η_3 is the range ratio of the third correlation range a_3 (*i.e.*, perpendicular to the a_2 and a_3) divided by a_1.

3.2Bayesian framework

A Bayesian framework is designed to assimilate prior knowledge $p(\psi)$, borehole testing data z_a, and long-term monitoring data z_b, for inferring SRFs, $\psi(x)$. Accordingly, the Posterior distribution, $p(\psi|z_a,z_b)$ is derived from Eq.(7),

$$p(\boldsymbol{\psi}\mid \boldsymbol{z}_a,\boldsymbol{z}_b)=\frac{L(\boldsymbol{z}_b\mid\boldsymbol{\psi},\boldsymbol{z}_a)p(\boldsymbol{\psi})}{\int_{\psi}L(\boldsymbol{z}_b\mid\boldsymbol{\psi},\boldsymbol{z}_a)p(\boldsymbol{\psi})d\boldsymbol{\psi}} \tag{7}$$

where, likelihood function, $L(z_b|\psi,z_a)$ is a probabilistic distribution of long-term monitoring data z_b, which is also subject to borehole testing data z_a, prior distribution $p(\psi)$, and soil-fluid coupling model $M(\psi,z_a)$. It is worth noting that posterior distribution $p(\psi|z_a,z_b)$ will take testing uncertainties, ε_a and ε_b into a further discussion.The analysis consists of three components: prior distribution, likelihood function, and posterior distribution.

3.2.1 Prior distribution

Before taking any on-site observations (*e.g.*, z_a and z_b) into the Bayesian framework, prior distribution $p(\psi)$ summarizes the knowledge that is available for SRFs (Wang *et al.*, 2013; Phoon *et al.*, 2016). Accordingly, the multivariate logarithmic normal distributionis generalized to depict number m geotechnical parameters at n spatial points as shown in Eq.(8),

$$p(\boldsymbol{\psi})=|\boldsymbol{C}|^{-\frac{1}{2}}(2\pi)^{-\frac{m\times n}{2}}\exp\left[-\frac{1}{2}(\ln\boldsymbol{\psi}-\boldsymbol{\mu})^T\boldsymbol{C}^{-1}(\ln\boldsymbol{\psi}-\boldsymbol{\mu})\right] \tag{8}$$

where C is the covariance matrix of SRFs, $\boldsymbol{C}=\boldsymbol{R}_n\otimes\boldsymbol{C}_m$, $\boldsymbol{C}_m$ is the covariance matrix of number m normal Random Variables (RVs),matrix R_n consists of autocorrelation and cross-correlation functions $\rho_{i,j}(h)\ (i,j=1,...,m)$,symbol '$\otimes$' denotes the operator of matrix multiplication. In a special scenario, lag distance $h=0$, which means that SRFs degenerate into RVs. Pearson correlation between two logarithmic normal RVs is represented by $\tau_{i,j}$, which equals to $\rho_{i,j}(h=0)\ (i,j=1,...,m)$ of SRFs.

3.2.2 Likelihood function

SRFs-based Bayesian method can assimilate prior knowledge $p(\psi)$, borehole testing data z_a, and long-term monitoring data z_b to obtain the posterior distribution of the key geotechnical parameters, $\psi=[c',\varphi',E,k_s]$. Likelihood function calculation includes two key components, general driver of soil-fluid coupling model $M(\psi,z_a)$ and multivariate discretization of SRFs.The following 5 key steps involve the conditional multivariate discretization.

(1) Defining a random path on the stochastic elements, each midpoint of an element is traversed once in a realization, the element edge size is less than the smallest correlation range, which guarantees to depict the spatial variation. Conditional data consist of the borehole testing data, z_a (*i.e.*, errors ε_a are randomly added to the observations), and the existing discretization $\psi(x_1),...,\psi(x_{i-1})$.

(2) Predicting the mean values $\mu_1(x_k)$ and $\mu_2(x_k)$, and the SD values $v_1(x_k)$ and $v_2(x_k)$, at the midpoint, x_k. The

recognized quantities include prior mean values, μ_1 and μ_2, SD values v_1 and v_2, autocorrelation function $\rho_{1,1}(h)$, $\rho_{2,2}(h)$, and cross-correlation function $\rho_{1,2}(h)$. Conditional data consist of the original borehole testing data z_a, and the discretized samples $\psi(x_1),...,\psi(x_{i-1})$.

(3) Building two normal distributions with $N[\mu_1(x_k),v_1^2(x_k)]$ and $N[\mu_2(x_k),v_2^2(x_k)]$ for the midpoint x_k, and taking one sample, respectively. The outcomes, $\psi_1(x_k)$ and $\psi_2(x_k)$ will be served as the new conditional data of the next midpoint x_{k+1}.

(4) Moving to the next midpoint x_{k+1} and then repeating steps 2 and 3 until sampling for all the stochastic elements.

(5) Finishing one multivariate discretization of SRFs, then backward transforming $\psi(x)$ with the exponential operator. Stochastic analysis of soil-fluid coupling model $M(\psi,z_a)$ will provide the theoretical results of long-term monitoring data z_b on a reservoir slope. Accordingly, the likelihood function $L(z_b|\psi,z_a)$ can be constructed for $\varepsilon_b = z_b - M(\psi,z_a)$, which is expressed by a multivariate normal distribution as shown in Eq.(9),

$$L(z_b|\psi,z_a)=\frac{\exp[-\frac{1}{2}(z_b-M(\psi,z_a))^T C_{\varepsilon_b}^{-1}(z_b-M(\psi,z_a))]}{\sqrt{(2\pi)^k|C_{\varepsilon_b}|}} \tag{9}$$

where, C_{ε_b} is the covariance matrix of the monitoring error ε_b, $|C_{\varepsilon_b}|$ is the determinant of C_{ε_b}.Furthermore, the correlation coefficient ω_{ij} ($i,j=1,...,k$) among ε_b is simplified into the function of mutual distance(Bhattacharjee, 2014) as shown in Eq.(10),

$$\omega_{ij}=1-\frac{D(x_i,x_j)}{\max D} \tag{10}$$

where $D(x_i,x_j)$ is the Cartesian distance between two monitoring points x_i and x_j, $\max D$ is the maximum distance of all the monitoring points.

3.2.3 Posterior distribution

Stochastic analysis of soil-fluid coupling mechanics $M(\psi,z_a)$ will consume a lot of computational resources. In the current analysis, Markov Chain Monte-Carlo (MCMC) simulation is used to fast obtain numerical solution.

Preparing the logarithmic normal prior distribution, $p(\psi=[c',\varphi',E,k_s])$ for SRFs, which includes the mean value vector μ, covariance matrix c. Taking out the i^{th} multivariate discretization of $\psi^i(x)$ subject to the prior distribution $p(\psi)$ and the originally conditional data z_a. Predicting the long-term measurements z_b using the stochastic analysis of soil-fluid coupling model, $M(\psi^i,z_a)$, and calculating the threshold, $\gamma_i=\min(\frac{L(z_b|\psi^i,z_a)p(\psi^i)}{L(z_b|\psi^{i-1},z_a)p(\psi^{i-1})},1)$. Taking a random sample u between 0 and 1, and comparing it with γ_i. If $\gamma_i>u$, accepting the spatial discretization $\psi^i(x)$ to be the posterior sample. Updating regularly the prior mean value vector μ, covariance matrix c from the accepted posteriorsamples for acceleration purposes, Reaching to the maximum samples, $i\le N$, and calculating the posterior distribution of $p(\psi|z_a,z_b)$.

4 Case studies

Shiliushubao slope has been stabilized since the original failure in the year 1975 as shown in Figure 1, which is currently reactivated after the impoundment of the Three Gorges Reservoir in Hubei Province, China.

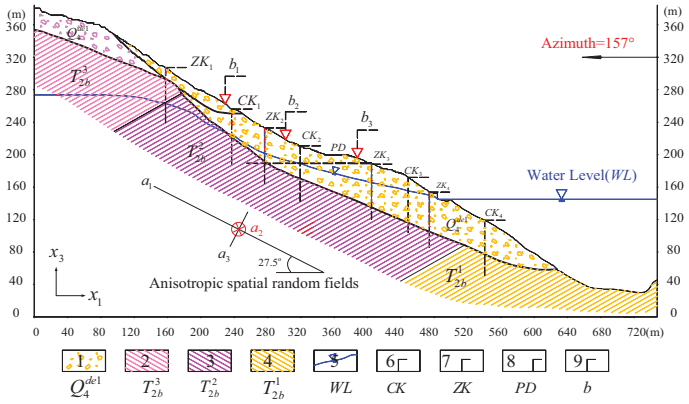

Figure 1. potential landslide section of the Shiliushubao slope

Geotechnical investigation indicates that the volume of the potential landslide body reaches 11.8×106m^3, and the slip area is 0.25km^2. The average longitudinal length and thickness reach 550m and 47m, respectively. Width is between 350m and 470m.Elevation varies between 60m and 350m, and the slope angles are 25°-45°.The report shows that the first water impoundment of the Three Gorges Reservoir was started from the initial

water level of 68m on May 25, 2003. Water level was reached its designed maximum of 175m in the year 2010. Since then, the water level of the reservoir has been periodically fluctuating between 145 and 175 m.

4.1 Engineering information

Posterior distributions of the key geotechnical parameters are applied to the reliability analysis of slope stability, which will take a landslide hazard prediction during an unprecedented heavy rainfall in the upcoming summer. Geotechnical investigation of the landslide deposit (*i.e.*, colluvial soil) provides the basic information of the key geotechnical parameters, such as the effective cohesion c', effective internal friction angle φ', Young's modulus E, and the saturated hydraulic conductivity k_s.The simulation parameters of the landslide sediment are set as follows, $\gamma=22$, $\nu=0.3$, $c'=39.8$, $\varphi'=35.4$, $E=99.9$, $k_s=2.41$.The simulation parameters of bedrock are set as follows, $\gamma=25$, $\nu=0.22$, $c'=1000$, $\varphi'=45$, $E=23170$, $k_s=0.25$. $ZK_1 \sim ZK_4$ provide the borehole testing data, such as the effective cohesion c', its mean value equals to 39.8kPa, mean value of the effective internal friction angle φ' equals to 35.4°. Exploratory adit PD only provides the data of Young's modulus E, and the mean value equals to 99.9MPa. Hydrogeological boreholes consist of $CK_1 \sim CK_4$, where the mean value of saturated hydraulic conductivity k_s, is 2.408m/d. There are three long-term monitoring points, b_1, b_2 and b_3 installed on the slope surface as listed in Table 1, which are used to collect slope settlements along with the periodic fluctuation of the reservoir water level and the amounts of annual rainfall, as shown in Figure 2. Monitoring errors ε_b are denoted into δ_b =0.1~0.3. Correlation coefficient, ω_{ij} among z_{b_1}, z_{b_2} and z_{b_3} is determined by the Cartesian distance, $i,j=1,2,3$.Hydrogeological properties are depicted by the SWCC that shows the curve between matric suction u_a-u_w and volumetric water content θ in Figure 3

Table 1. Long-term monitoring data of the reservoir slope surface

Point	Coordinates		Long-term monitoring data				
	X_1(m)	X_3(m)	Three-months settlement (mm)				δ_b
b_1	301.8	217.8	130	107	128	111	0.1~0.3
b_2	342.5	200.1	108	103	109	99	0.1~0.3
b_3	388.7	196.2	67	66	66	72	0.1~0.3

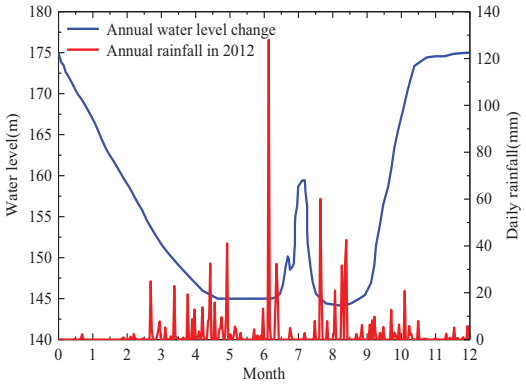

Figure 2. Hydraulic boundary conditionsfor theunsaturated transient seepage

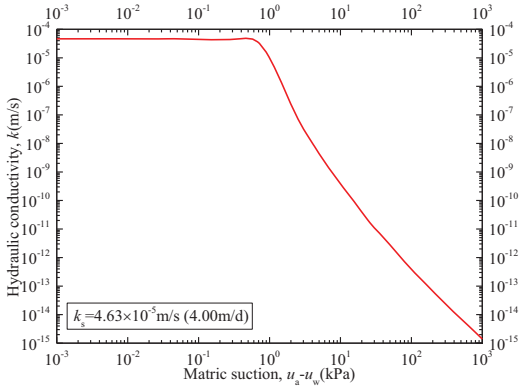

Figure 3. Hydraulic Conductivity Function (HCF) between matric suction and water content.

4.1.1 Prior knowledge

Borehole testing data of Table 1 cannot provide comprehensive statistics for the SRFs, $\psi=[c',\varphi',E,k_s]$, but a scope denotes the magnitudes of the key geotechnical parameters. Thus, prior distribution of ψ is proposed to be a multivariate of Logarithmic Normal (*LN*) distribution with large uncertainty. In this condition, the Marginal distribution, c' is subject to $LN(50,50^2)$kPa, φ' is subject to $LN(40,40^2)$°, E is subject to $LN(120,120^2)$MPa, and k_s is subject to $LN(4.0,4.0^2)$m/d. Correlation coefficient, $\tau_{ij},i,j=1,...,4,\ i\neq j$ is assumed to be 0.0 at the beginning of the joint prior distribution. According to the landslide formation mechanism (Jian *et al.*, 2014), the first correlation range of the geotechnical parameters ψ is proposed to be parallel with the slope surface (*i.e.*, the angle of dip equals to 27.5°). The second correlation range is perpendicular to the first one, and a_1 and a_2 are assumed to be 20m each. The initially third range ratio is postulated to be, $\eta_{c',3}=\eta_{\varphi',3}=\eta_{E,3}=\eta_{k_s,3}=0.2$.

4.1.2Posteriors of the key geotechnical parameters

The joint prior distribution $p(\psi)$ took a total of 1,000 Markov chain spatial discretization, which consumed 22 hours of stochastic analysis on a workstation of CPU Intel i9 @ 10 cores.The posterior statistical results for the geotechnical parameters are shown in Table 2.

Table 2. Logarithmic normalposterior distributions of the SRFs

Geotechnical parameter	Mean value	SD value	Correlation ranges		Correlation coefficient τ			
			$a_1 = a_2$ (m)	η_3	c' (kPa)	φ' (°)	E (MPa)	k_s (m/d)
c' (kPa)	35.075	4.275	20.0	0.230	1.0	-0.040	-0.055	-0.049
φ' (°)	30.075	2.617	20.0	0.296	-0.040	1.0	0.047	0.199
E (MPa)	94.800	13.044	20.0	0.313	-0.055	0.047	1.0	0.100
k_s (m/d)	2.042	0.292	20.0	0.267	-0.049	0.199	0.100	1.0

4.2Reliability analysis of slope stability

Heavy rainfall outlines a major threat to the Three Gorges Reservoir area in the month of July each year. The above calibrated geotechnical parameters are used to analyze the reliability index of the slope stability. SRFs have two outstanding advantages than RVs. The former can provide more precise sliding trajectory and accurate reliability index than the latter. For instance, the slope stability is analyzed in the case of an average reservoir water level of 152m and a heavy rainfall of 100mm/d for five consecutive days in the upcoming summer, which becomes risky for the safety of life and property of the local residents. Figure 4 shows a pseudo scenario in which if particularly 100kPa of strength is added to effective cohesion c' at boreholes ZK_1 and ZK_2, the critical slip surface #1 (*i.e.*, slip radius=948.42m) will be replaced by the second slip surface #2 (*i.e.*, slip radius=468.13m) using SRFs. Therefore, the slip surface #1 controls the slope stability. In the following sub-sections, the factor of safety, FOS, and the reliability index are discussed using assumptions of RVs and SRFs, respectively.

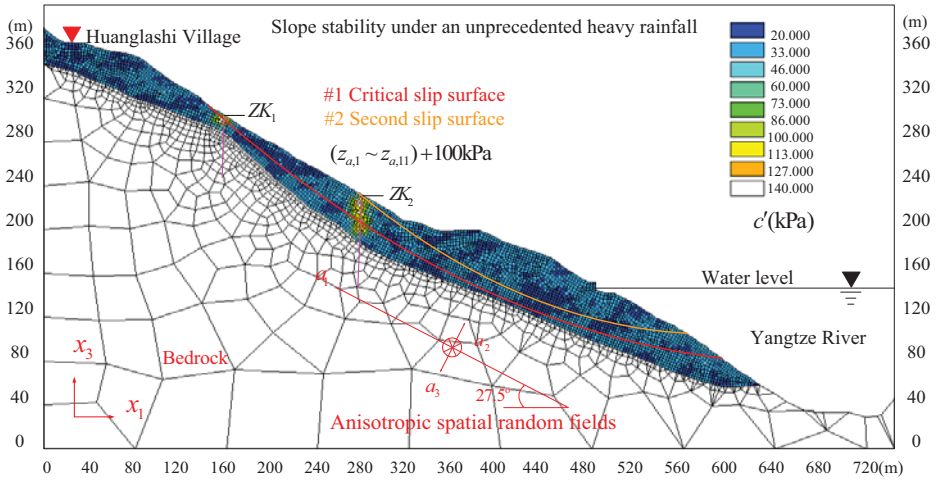

Figure 4. Variation of the critical slip surface under effective cohesion c' (kPa) according to SRFs assumption

4.2.1 Reliability results of SRF assumption

(1) Reliability results in the common years

Reliability analysis employed by SRFs takes the spatial variability of the key geotechnical parameters into account, and thus this approach guarantees the finding of a more precise and coherent reliability index of the FOS.

SRFs use SMC algorithm to calculate the reliability index β, two subset parameters are needed, subset number N and p_0. The analysis is free in the choice of failure ratio p_0, and the subset number N. However, N should be selected large enough to give an accurate estimate of p_0. Let N change from 100 to 1500, and let p_0 equals 0.05, 0.10 and 0.15, respectively. Accordingly, there are two zones of reliability index β as shown in Figure 5, the left one is the unstable combination until $N = 1000$, whereas the right one remains stable combination. In this case, for the purpose of balancing the precision and the efficiency, $N = 1000$ is chosen as the optimal parameter. β_{SRF} achieves the maximum subject to $p_0 = 0.10$. Reliability index of FOS is $\beta_{SRF} = 2.470$, and the corresponding failure probability P_f equals to 0.7%. SMC algorithm only takes 3,000 stochastic simulations, which consume 1/3 times more when contrasted with the classical MC algorithm.

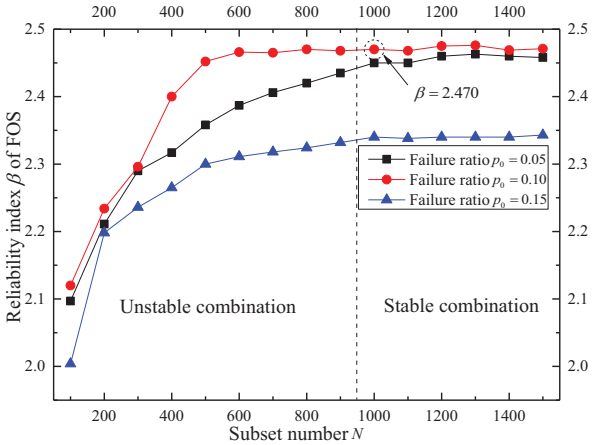

Figure 5. Reliability index of the slope stability per SMC algorithm

(2) Reliability results in the specific year of 2020

In August 2020, the 5th flood wave of the Yangtze River passed through the Three Gorges reservoir area accompanied by heavy rainfall in China. The reservoir water level varies with 15 m during 6 days. The complex working condition will lead to the resurgence of old landslides. The predicted results will be highly biased using only the safety factor as the evaluation indicator. An unsaturated slope reliability analysis method is based on the strong hydraulic disturbance in the Three Gorges reservoir area, which considers the randomness of Soil-Water Characteristic Curve (SWCC) and the spatial variability of saturated hydraulic conductivity. At first, Parameters and uncertainties of SWCC model VGM, VGB, VG and FX are calibrated by a Bayesian approach, and then spatial random field of the saturated hydraulic conductivity are discretized in the sliding body. Finally, the reliability analysis will calculate the failure probability of the reservoir bank slope only considering the random characteristics of the SWCC models, and the reliability index resulting of the spatial variability of the unsaturated hydraulic conductivity.Figure 6 shows the reliability index of slope stability corresponding to the SWCC models，the FX model corresponds to the smallest reliability indicator, β=2.741, and the VGB model corresponds to the largest reliability indicator, β=3.641. The results show that using the unsaturated hydraulic conductivity as a random variable, the calculated reliable index cannot meet the requirements in the specification (β<2.70). The method is applied to Shiliushubao slope of the Three Gorges Reservoir area. The safety factor of slope stability is lowunder rapid water level fluctuations and heavy rainfall, but the reliability index meets the requirement of the code. None of the additional reinforcement measures are required.

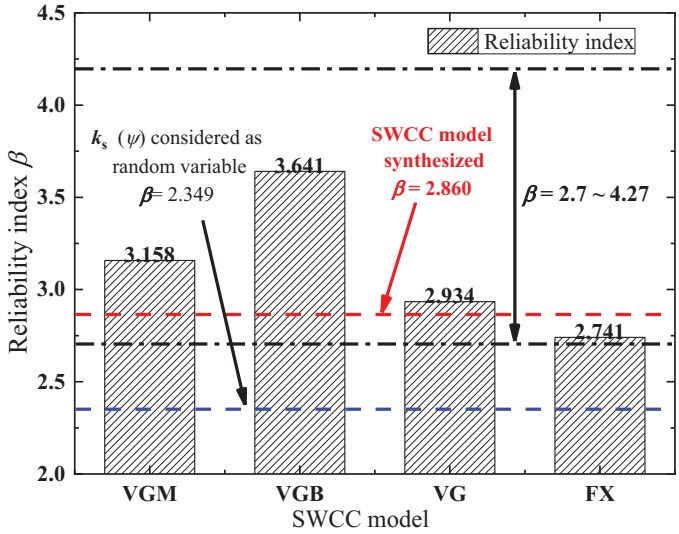

Figure 6. Reliability indicators of different SWCC models

5 Conclusions

Spatial random fields-Bayesian method is innovatively designed for the reliability analysis of unsaturated soil slope. The following conclusions are drawn.

Four key geotechnical parameters c',φ',E and k_s are calibrated quarterly by integrating the prior knowledge, borehole testing data, and long-term monitoring data of the year 2012. All the posterior mean values are less than the priors, which indicates that using the borehole testing data directly will be a risky.

Factor of safety, FOS, of the once failed slope is concentrated within the range of 1.1~1.5. During an unprecedented heavy rainfall for the upcoming summer, the deterministic FOS is $F_s = 1.055$, which is subject to the posterior mean values $c' = 35.075\text{kPa}$, $\varphi' = 30.075°$ and $k_s = 2.042\text{m/d}$. The impacts of the geotechnical parameters, in the order of from the largest to the smallest, are φ' (*i.e.*, 72%), c' (*i.e.*, 18%), and k_s (*i.e.*, 10%).

Assumption of random variables will underestimate the reliability index β of the reservoir slope. The result $\beta_{RV} = 0.622$ indicates that rescue treatments are necessary for slope reinforcement. Reliability index β_{SRF} will increase to 2.470 adopting the assumption of spatial random fields, which is a more practical result because it takes the spatial variability of the key geotechnical parameters into account.

Spatial random fields-based Bayesian method can prove that it is unnecessary to adopt additional strengthening treatments to prevent Shiliushubao landslide under an unprecedented heavy rainfall for the upcoming summer. However, it is recommended that long-term monitoring system should be continued to provide more reliable and sustainable measurements.

References

Au S, Beck JL(2001) Estimation of small failure probabilities in high dimensions by subset simulation. *PROBABILISTIC ENG MECH* 16: 263-277.

Au S, Wang Y (2014) Engineering risk assessment with subset simulation. *John Wiley & Sons Singapore*.

Cai JS, Yan EC, Yeh TC J, Zha YY, Liang Y, Huang SY, Wang WK, Wen JC (2017) Effect of spatial variability of shear strength on reliability of infinite slopes using analytical approach. *COMPUT GEOTECH* 81:77-86.

Ching JY, Au SK, Beck JL(2005) Reliability estimation for dynamical systems subject to stochastic excitation using subset simulation with splitting. *COMPUTER METHODS IN APPLIED MECHANICS AND ENGINEERING* 194: 1557-1579.

De Vita P, Reichenbach P, Bathurst JC, Borga M, Crosta G, Crozier M, Glade T, Guzzetti F, Hansen A, Wasowski J (1998) Rainfall-triggered landslides: a reference list. *ENVIRON GEOL* 35: 219-233.

Huang QX, Wang JL, Xue X (2016) Interpreting the influence of rainfall and reservoir infilling on a landslide. *LANDSLIDES* 13: 1139-1149.

Jian WX, Xu Q, Yang HF, and Wang FW (2014) Mechanism and failure process of Qianjiangping landslide in the Three Gorges Reservoir, China. *ENVIRON. EARTH SCI* 72: 2999-3013.

Lo MK, Leung YF (2019) Bayesian updating of subsurface spatial variability for improved prediction of braced excavation response. *CAN GEOTECH* J 56: 1169-1183.

Low BK, Tang WH (2007) Efficient spreadsheet algorithm for first-order reliability method. *J ENG MECH ASCE* 133: 1378-1387.

Lu N, Godt JW, Wu DT (2010) A closed-form equation for effective stress in unsaturated soil. *WATER RESOUR RES* 46: W05515.

Matheron G, Armstrong M (1963) Principles of geostatistics. *ECON GEOL* 58: 1246-1266.

Phoon KK, Prakoso W A, Wang Y, Ching JY (2016) Uncertainty representation of geotechnical design parameters. Chapter 3. In Reliability of geotechnical structures in ISO2394, pp 49-88.

Richards LA (1931) Capillary conduction of liquids through porous mediums. *J PHYS* 1: 318-333.

Tandjiria V, Teh CI, Low BK (2000) Reliability analysis of laterally loaded piles using response surface methods. *STRUCT* SAF 22: 335-355.

Van Genuchten, MT (1980) A closed-form equation for predicting the hydraulic conductivity of unsaturated soils. *SOIL SCI SOC AM J* 44: 892-898.

Wang Y, Huang K, Cao ZJ (2013) Probabilistic identification of underground soil stratification using cone penetration tests. *CAN GEOTECH J* 50: 766-776.

Zheng D, Huang JS, Li DQ, Kelly R, Sloan SW, (2017) Embankment prediction using testing data and monitored behaviour: A Bayesian updating approach. *COMPUT GEOTECH* 93: 150-162.